Complex Permittivity Measurements with Quasioptical Fabry-Pérot Resonators

B. D. Elwood^{1,2,*}, P. K. Grimes¹, and J. M. Kovac^{1,2}

Abstract. As millimeter instrumentalists push the precision and mapping speed of their instruments ever-higher to make ever-deeper measurements, the need for a precise understanding of the complex permittivity of the dielectrics used in these instruments at their operating temperature heightens. To address this need, we have developed high quality factor quasioptical Fabry-Pérot open resonators spanning 75 GHz-330 GHz, optimized for rapid use in a quick-turnaround 4 K cryostat. These hemispherical resonators enable precise metrology of low-loss bulk and thin dielectrics. We present the design and characterization of, and some complex permittivity measurements from, a W-band open resonator.

1 Introduction

The need for rapid, precise characterization of dielectrics near realistic operating conditions has become apparent in CMB polarimeters that employ cryogenic refractive optics—such as the current and upcoming BICEP instruments—since losses in transmissive optics elevate photon noise, degrading mapping speed and overall sensitivity, and possible scattering from commonly employed foam materials can additionally contribute to undesired environmental coupling. Meeting the stringent demands of these high-contrast, high-throughput imaging systems requires a precise understanding of the complex permittivity of the dielectrics that compose their optics, including laminates and bulk materials. This understanding in turn guides the choice of material for and design of optical components ranging from anti-reflection coatings to refractive elements and radio-transparent multi-layer insulation [1].

Rapid, precise measurements of complex permittivity can accelerate informed material selection in millimeter-wave optics. This capability also has applications in the development of wider mm-wave instrumentation efforts, for example in black-hole imaging experiments, line-intensity mapping, mm-wave cavity axion searches, or sub-mm surveys [2, 3]. In this work, we introduce and validate an approach based on quasioptical Fabry-Pérot resonators, enabling rapid and precise broadband characterization of low-loss materials.

2 Apparatus & Procedure

The mode structure of open resonators contains information about cavity length and loss. Open resonators have the advantage of being inherently broadband, and suffer less from systematics related to sample dielectric dimensions than closed waveguide techniques. Whereas

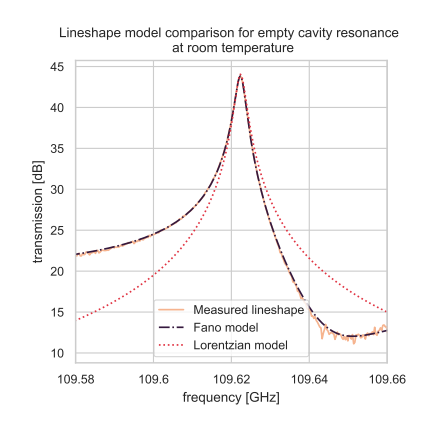
¹Center for Astrophysics | Harvard & Smithsonian, Cambridge, MA 02138, USA

²Department of Physics, Harvard University, Cambridge, MA 02138, USA

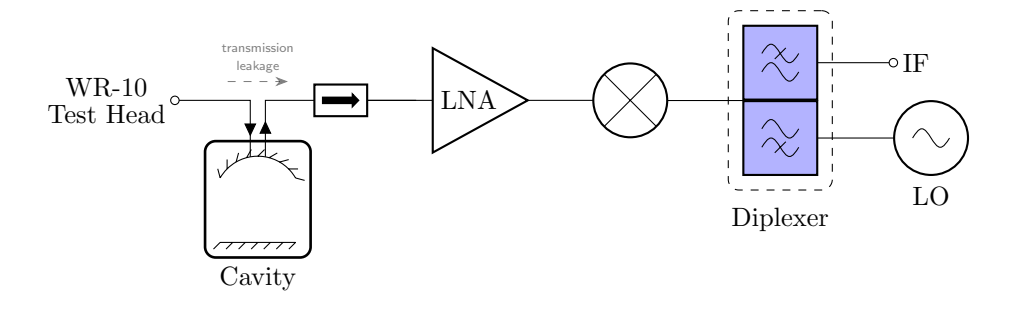
^{*}email: bdelwood@fas.harvard.edu



(a) Cavity placed in a quick-turnaround cryostat for cryogenic measurements. We couple in radiation via stainless steel waveguides to decrease thermal conduction from ambient temperature to the cold stages. The cold plate is thermally strapped to the second stage of a PT405 pulse tube cryocooler to cool the cavity down to $4\,\mathrm{K}$. A $50\,\mathrm{K}$ radiation shield reduces loading on the second stage.



(b) An example resonance mode measurement (solid peach) overlaid with a best-fit Fano (dash-dot purple) and Lorentzian (dotted red) lineshapes. Note that the asymmetry in the mode due to complex coupling is captured well by the Fano model.



(c) Schematic diagram of the signal chain for W-band measurements [4].

Figure 1. The Fabry-Pérot resonator employed for this work (a), an example empty cavity measurement (b), and the W-band signal chain (c).

closed waveguide techniques require fabricating multiple samples to span different waveguide dimensions, open-resonator methods allow the same dielectric samples to be used across all bands. Open resonators also permit direct measurement of birefringence via mode splitting, which results from breaking the degeneracy between the polarization eigenstates of the fundamental modes when the cavity is loaded with a birefringent material [5].

The resonator used for this work is constructed from gold-plated planar and spherical high-purity copper mirrors, separated by Invar struts, which form a hemispherical near-confocal resonator. A VNA extension head couples radiation into the cavity via a split-block waveguide butted into a recess in the top (spherical) mirror. The coupling apertures are sized such that the intrinsic cavity quality factor is $O(1 \times 10^5)$. A custom receiver composed of an

isolator, LNA, and mixer enables S_{21} measurements. The W-band cavity used for the measurements reported in this work has a length of 55 mm and a mirror radius of curvature of 100 mm, giving a free spectral range of approximately 2.7 GHz. A modular design allows wideband operation by requiring only the replacement of the VNA extension head, spherical mirror, coupling block, and receiver between bands. We have a range of VNA extension heads, coupling blocks, spherical mirrors, and custom receivers for operating cavities from 75 GHz-330 GHz. For loaded cavity measurements, a dielectric sample is pressed against the flat mirror. See Fig. 1 for details on the apparatus.

Inferring loss tangent from a loaded open resonator requires carefully measuring resonance mode frequencies (a measure of cavity length, including sample electrical length) and quality factors (a measure of the energy stored in a given mode). There are two measurement techniques for measuring index and loss tangent: frequency-variation and length-variation [6]. In both methods, we sweep in frequency across the band and record the cavity response. In the frequency-variation method, we fix the cavity length. The modes shift in frequency when the cavity is loaded. With length-variation, we tune the loaded cavity by adjusting cavity length to move the resonances back to their unloaded frequency. The former approach suffers less from systematic error in measurements of index. The latter is more advantageous for measuring $\tan \delta$, as the frequency dependent coupling factor $\beta(k)$ – and therefore the intrinsic quality factor $Q_0(k)$ – remains identical in the loaded and unloaded cavities. For both methods:

- 1. Measure the fundamental mode frequencies and quality factors. Determine the cavity length and mirror radius of curvature from the mode frequencies.
- 2. Load the cavity with a sample and measure the fundamental modes.
- 3. In the frequency-variation method, infer the sample electrical length from the shift in mode frequencies. With length modulation, the length change required to retune the cavity gives the sample electrical length.
- 4. From the empty cavity quality factors, loaded quality factors, and sample electrical length, compute material loss with Eqn. (1).

We compute the loss tangent as [7]

$$\tan \delta = \frac{1}{Q_s} \frac{2nk(t\Delta + d)}{2nkt\Delta - \Delta \left[\sin\left(2(nkt - \Phi_D)\right)\right]},\tag{1}$$

where $\frac{1}{Q_s} = \frac{1}{Q_L} - \frac{1}{Q_0(k)}$ and $\Delta \equiv \frac{n^2}{n^2\cos^2(nkt-\Phi_T)+\sin^2(nkt-\Phi_T)}$, with Q_L the loaded quality factor, n the index of refraction, t the sample thickness, and k the wavenumber in the material. In the loaded cavity, the wavefront curvature at the mirror and sample interfaces does not match, which shifts the loaded cavity modes relative to a cavity filled with an idealized dielectric of the same effective index and loss, which is an assumption from which Eqn. (1) is derived. Thus, the measured mode frequencies, $f_{L,i}$, need to be corrected for these effects before computing $\tan \delta$:

$$f_{L} = f_{L,i}(1 + f_{\text{interface}} + f_{\text{mirror}})$$

$$= f_{L,i} \left(1 + \frac{t(n-\Delta)}{n^{2}k^{2}\omega_{i}^{2}(t\Delta+d)} + \frac{3}{4k^{2}(t\Delta+d)R} \right), \tag{2}$$

where d is the free-space cavity length, R the mirror radius of curvature, and ω_t the beam waist at the dielectric interface.

In general, we utilize the frequency-variation method, as it does not require precisely controlling the length of the cavity. We can account for the quality factor frequency variation by taking measurements mapping its trend across the band and using the interpolated intrinsic quality factor when calculating loss tangent. Fig. 2a shows the intrinsic Q_0 with the interpolated values used for the HDPE measurements. We infer Q_0 by fitting a four-parameter Fano lineshape to each fundamental mode observed in the unloaded, empty cavity. We use a Fano lineshape rather than a Lorentzian as the phasing of the transmission leakage interacting with the cavity resonance modes leads to asymmetry in the transmission profile, which is accounted for in the complex coupling coefficient in the Fano model. Fig. 1b shows an example of a resonance mode with the Lorentzian and Fano best-fit models.

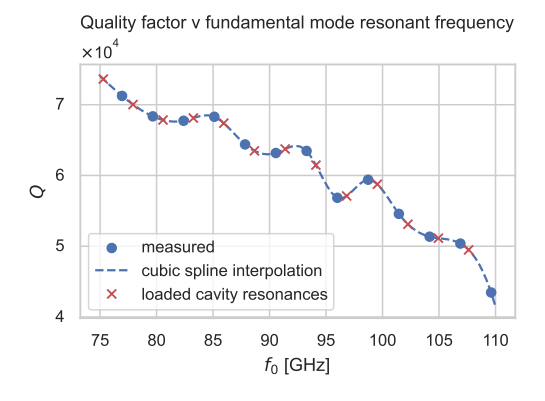
Likewise, we need to understand the intrinsic quality factor down to 4 K, as this apparatus is designed for cryogenic index and loss measurements. Cavity loss evolves as a function of temperature for several reasons. As the cavity cools, the dimensions of the coupling block change, altering the coupling aperture size, aperture spacing, and the coupler-mirror interface spacing and pressure, perturbing the coupling factor β . Cavity contraction shifts resonance modes, changing their coupling factor; although this should be a subdominant effect, as the shifts are small and the $Q_0(k)$ curve is slowly-varying. Finally, the surface resistivity of the mirrors generally decreases at colder temperatures, driving up Q.

The background of the resonance mode measurements is dominated by direct transmission from the transmit port to the receive port, depicted in Fig. 1c as "transmission leakage" across the cavity. Fig. 2b demonstrates that this transmission leakage is not a product of direct leakage across the apertures on the face of the spherical mirror; this leakage comes from coupling between the apertures of the waveguide-mirror coupling block. This understanding led us to initially expect that the dominant change in the cavity mode structure during cooldown would be due to variations in the background leakage levels from mechanical changes at the coupling block-mirror interface. Specifically, these variations would arise from changes in pressure and spacing at the coupler-mirror interface, which modify the electromagnetic choke between the split-block waveguide coupler and mirror.

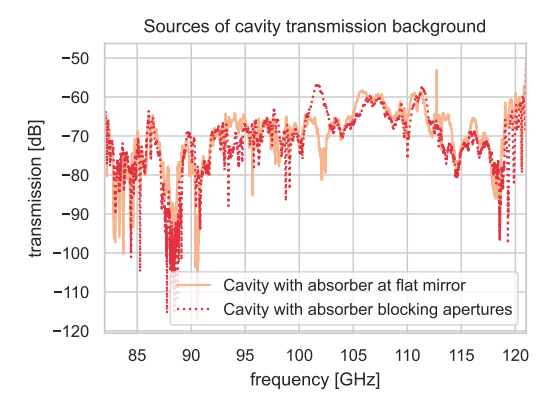
However, we observed that the transmission background did not change significantly after the cooldown. In fact, tracking a single mode during unloaded cavity cooldown, the Q rises by 30.4% (Fig. 2c). This effect appears consistent with reduced mirror surface resistivity. Additionally, given the construction of the coupling block-mirror interface, excess pressure on that interface (which may be caused by differential contraction between the mounting hardware and the coupling block material) can distort the mirror. These distortions will couple power out of the fundamental modes into the higher order modes. Through several cooldown cycles we did not see evidence of mirror-distortion induced higher order mode structure, nor did we observe additional mirror distortions immediately after thermal cycling.

3 Results

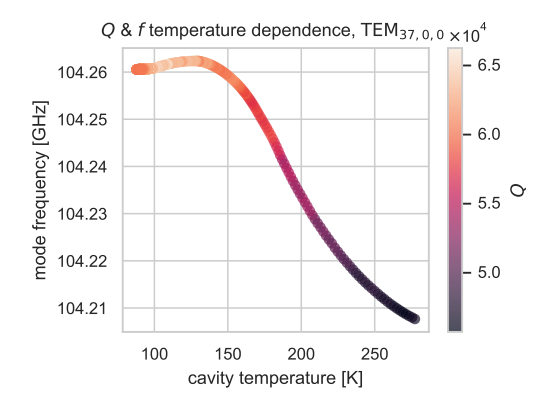
Utilizing the frequency-variation method, we obtain W band (75 GHz-110 GHz) measurements of the index of refraction and loss of several materials common in mm-wave instrumentation, which are reported in Table 1. The reported uncertainties include variations in the mode quality factor and inferred electrical length by measuring the 13 axial modes in the W band. We also account for systematics due to the measurement procedure by taking multiple measurements of the sample at different orientations and clamping pressures, which helps to control for effects due to sample surface roughness or curvature. As a cross-check for the interface correction (Eqn. (2)), we generally take measurements of several thicknesses of the same material.



(a) The intrinsic cavity quality factor across the WR-10 band at room temperature. The overall downward trend occurs because the nearfield attenuation of the evanescent mode coupling of the apertures decreases with frequency, increasing the coupling level. We take the Q_0 in the frequency-variation method from this interpolation.



(b) Broadband scan of the W-band cavity at room temperature. In one scan (peach), the cavity is dampened by an absorber at the flat mirror, while in the other scan (dotted red) an absorber is placed between the coupling apertures on the front side of the spherical mirror. If the background leakage was dominated by coupling between the apertures at the spherical interface, we would expect these two spectra to deviate on the order of 20 dB across the band.



(c) Mode frequency and quality factor for an unloaded cavity during cooldown for a single axial mode. The shift in resonance frequency indicates a length contraction of 15 μ m, consistent with the expected contraction of the Invar struts. The Q of the mode increases $\approx 30\%$, attributed to decreased mirror surface resistance.

Figure 2. Characterization measurements of the W-band cavity: (a) Intrinsic quality factor as a function of frequency (b) Broadband transmission with absorbers at different locations; and (c) Mode frequency and *Q* during cavity cooldown.

Table 1. Indices and losses of several materials at room temperature. The HDPE, annealed HDPE, UHMWPE, and LDPE results were previously reported in [4]. The HDPE, annealed HDPE, and UHMWPE results are reported as the W-band average for 4 sample thicknesses [4]. A measurement of 25 μm thick LDPE is included to illustrate the capability of the cavity to measure thin, low-loss materials. The low-loss silicon results are again reported as the W-band average, but only for a single 3 mm sample. Loss is reported as power lost from the cavity in a single pass through the dielectric (through 2 mm for HDPE, annealed HDPE, and UHMWPE and through 3 mm for Si).

material	n	$\tan \delta \ (\times 10^{-4})$	loss (dB)
HDPE	1.537 ± 0.003	1.66 ± 0.18	-31
annealed HDPE	1.541 ± 0.004	1.48 ± 0.24	-32
UHMWPE	1.526 ± 0.007	1.43 ± 0.21	-32
LDPE			-52
low-loss Si	3.4230 ± 0.0001	1.47 ± 0.63	-30

4 Conclusions & Future Work

We present a case for the utility of mm-wave open resonators for taking broadband measurements of complex permittivity. We have reported progress on characterizing the unloaded W-band resonator at cryogenic temperatures, and reported index and loss measurements from that cavity at room temperature for samples of HDPE and low-loss silicon. We are conducting a measurement campaign targeting high-impact candidate materials for optical components in current and future BICEP instruments, with near-term results expected on the room-temperature optical properties of materials for RT-MLI, laminate windows, AR coatings, and birefringent materials for half-wave plate polarization modulators.

References

- [1] P.A.R. Ade et al., BICEP/Keck XIX: Extremely Thin Composite Polymer Vacuum Windows for BICEP and Other High Throughput Millimeter Wave Telescopes (2024), 2411.10428
- [2] M.D. Johnson *et al.*, Galaxies **11**, 61 (2023)
- [3] G. Hoshino *et al.*, Physical Review Letters **134**, 171002 (2025)
- [4] B.D. Elwood et al., Fabry-Pérot Open Resonant Cavities for Measuring the Dielectric Parameters of Mm-Wave Optical Materials, in Millimeter, Submillimeter, and Far-Infrared Detectors and Instrumentation for Astronomy XII (SPIE, 2024), Vol. PC13102, pp. 22–33
- [5] R.G. Jones, Journal of Physics D: Applied Physics 9, 819 (1976)
- [6] P.K. Yu *et al.*, Proceedings of the Royal Society of London. A. Mathematical and Physical Sciences **380**, 49 (1982)
- [7] T. Hirvonen *et al.*, IEEE Transactions on Instrumentation and Measurement **45**, 780 (1996)